Electrical Engineering

School of Engineering

12-1-2001

Spectroscopic ellipsometry and electrical studies of as-grown and rapid thermal oxidized $Si_{1-x-y}Ge_xC_y$ films

W. K. Choi

W. Feng

L. K. Bera

Cary Y. Yang
Santa Clara University, cyang@scu.edu

J. Mi

Spectroscopic ellipsometry and electrical studies of as-grown and rapid thermal oxidized $Si_{1-x-y}Ge_xC_y$ films

W. K. Choi,[a)] W. Feng, and L. K. Bera
Microelectronics Laboratory, Department of Electrical and Computer Engineering, National University of Singapore 4 Engineering Drive 3, Singapore 117576

C. Y. Yang and J. Mi
Microelectronics Laboratory, Santa Clara University, 500 El Camino Real, Santa Clara, California 95053

Transmission electron microscopy results showed the formation of SiC precipitation in a rapid thermally oxidized (RTO) $Si_{1-x-y}Ge_xC_y$ sample with high-C content. The spectroscopic ellipsometry results showed that the E_1 gap increased and E_2 gap decreased as the C concentration increased. For the oxidized samples, the amplitude of the E_2 transitions reduced rapidly and the E_1 transition shifted to a lower energy. The reduction in the E_2 transitions was due to the presence of the oxide layer. A high-Ge content layer and the low-C content in the RTO films accounted for the E_1 shift to lower energy. The electrical measurements showed that RTO at 800 °C did not improve the oxide quality as compared to 1000 °C. © *2001 American Institute of Physics.*
[DOI: 10.1063/1.1413715]

I. INTRODUCTION

Epitaxial $Si_{1-x}Ge_x$/Si heterostructures[1-4] have demonstrated impressive results for Si-based band-gap engineering. The incorporation of carbon (C) in $Si_{1-x}Ge_x$ layers allows the growth of heterostructures with well-controlled misfit strain. The growth of such layers is, however, difficult due to the high mismatch between C and Si lattices, low solubility of C in Si, and the tendency of silicon carbide precipitation.

We have recently carried out structural[5,6] and electrical[7] characterizations of as-grown and rapid thermal oxidized (RTO) $Si_{1-x-y}Ge_xC_y$ alloy films grown by rapid thermal chemical-vapor deposition (RTCVD). We found that C incorporation into the $Si_{1-x-y}Ge_xC_y$ system can lead to compressive or tensile strain in the film. For compressive or fully compensated films, the RTO process drastically reduces the C content such that the oxidized films closely resemble the $Si_{1-x}Ge_x$ films. For tensile films, two broad regions, one with carbon content higher and the other lower than that required for full compensation, coexist in the oxidized films. We have also reported briefly the formation of SiC precipitates in the high-C content RTO samples.

The electrical results of oxides grown at 1000 °C indicated segregation of Ge at the $SiO_2/Si_{1-x-y}Ge_xC_y$ interface, a thin GeO_2 layer at the oxide surface, and elemental Ge at the interface and in the oxide. Due to the segregation of Ge at the interface, a very high ($3-3.6 \times 10^{11} eV^{-1} cm^{-2}$) interface state density was obtained. All the oxides showed electron trapping behavior and the trap generation rate decreased with increasing C concentration. The charge-to-breakdown value and the oxide breakdown field were higher for $Si_{1-x}Ge_x$ than $Si_{1-x}Ge_xC_y$ samples, and these values decreased with increasing C concentration.

In this work, we investigate further the formation of SiC precipitates in $Si_{1-x}Ge_xC_y$ samples using transmission electron microscopy (TEM). We examine the influence of C on the film's optical properties by spectroscopic ellipsometry (SE). As the oxides grown at 1000 °C were shown to be unsatisfactory, we attempted to grow oxides at a lower RTO temperature of 800 °C in O_2 or N_2O. The electrical results of such oxides are reported in this article.

II. EXPERIMENT

The $Si_{1-x-y}Ge_xC_y$ samples were epitaxially grown on n-type (100) Si substrates by RTCVD.[8] The growth was achieved by heating the substrate with a bank of halogen lamps at 500–600 °C with a pressure of 1.5 Torr. A Si buffer layer (200 nm) was grown at 900 °C, followed by the growth of the alloy layer. The process gases were silane (SiH_4), germane (GeH_4), methylsilane ($SiCH_6$), and hydrogen (H_2). The alloy thickness was in the range of 50–130 nm.

Rapid thermal oxidation was achieved with an AST SHS 10 rapid thermal processor. Details of the RTO process can be found in our earlier article.[6] RTO was performed at 800 °C for 600 s in dry oxygen (O_2) or N_2O ambient. The oxide thickness was found to be between 4 and 5.5 nm. The TEM experiments were carried out using a Philips CM300 system with an operating voltage of 300 kV. The SE experiments were performed using a spectroscopic phase-modulated ellipsometer (UVSEL) with the energy ranged from 1.5 to 4.5 eV. The rotating polarizer and tracking analyzer were set at 70°. The energy increment and integration time were set at 0.01 eV and 2 s, respectively. The critical-point energy (E_{cp}) and broadening factor (Γ) were obtained by curve fitting the second derivative of the dielectric constant ($\epsilon = \epsilon_1 + i\epsilon_2$) versus energy plots using the least-square method.

The electrical properties of the oxides were investigated using the capacitance–voltage ($C-V$), conductance–voltage ($G-V$), and the current–voltage ($I-V$) characteristics of the $Al-SiO_2-Si_{1-x-y}Ge_xC_y$ capacitor structure. The $C-V$

a)Electronic mail: elechoi@nus.edu.sg
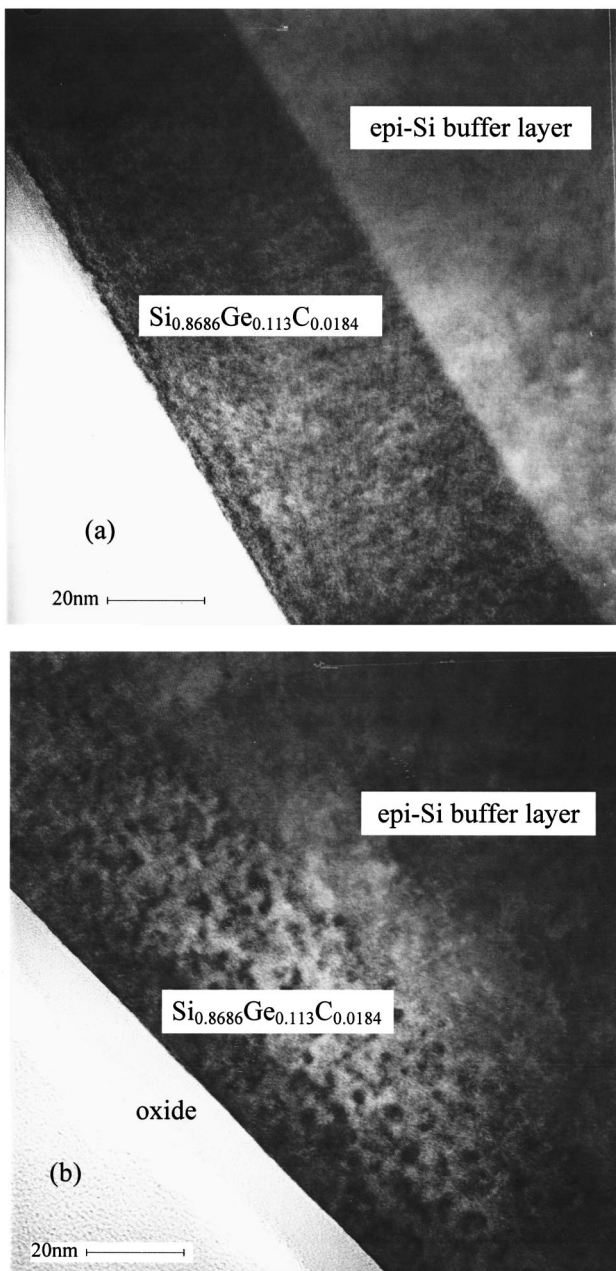
FIG. 1. Typical cross-sectional TEM micrographs of (a) as-grown and (b) rapid thermally oxidized $Si_{0.8686}Ge_{0.113}C_{0.0184}$ samples.

$(G-V)$ and the $I-V$ measurements were carried out using an HP4192 LF impedance analyzer and an HP4156 semiconductor parameter analyzer, respectively.

III. RESULTS AND DISCUSSION

A. TEM results

Figure 1 show typical TEM results of the as-grown and RTO $Si_{1-x-y}Ge_xC_y$ samples. Figure 1(a) shows a very good interface between $Si_{0.8686}Ge_{0.113}C_{0.0184}$ and the Si buffer layer. No microtwins or defects can be observed in the as-grown sample. Figure 1(b) shows that after RTO at 1000 °C, there is a lack of sharp interface between $Si_{0.8686}Ge_{0.113}C_{0.0184}$ and the Si buffer layer. This may be due

to Ge diffused into the Si substrate as a result of high-temperature oxidation. The whole $Si_{0.8686}Ge_{0.113}C_{0.0184}$ film is also found to contain a significant number of black spots. There are two TEM studies on SiC formation in SiGeC films.[9,10] The SiGeC samples of Warren *et al.*[9] (C=1%) and Cuadras *et al.*[10] (C=0.5%) exhibited very different SiC precipitate density. The precipitate density of Warren *et al.* is similar to our results of Fig. 1(b). It is useful to point out that Strane *et al.*[11] also reported a SiC precipitate distribution in an annealed (at 925 °C for 190 min) $Si_{0.986}C_{0.014}$ alloy, very similar to our results.

We have also observed from our TEM results of rapid thermally oxidized $Si_{0.8811}Ge_{0.113}C_{0.0059}$ and $Si_{0.8738}Ge_{0.113}C_{0.0132}$ samples that the SiC precipitates were significantly lesser than that shown in Fig. 1(b). The TEM results, therefore, agree with our IR results[6] in that the formation of SiC precipitates can only be observed in the high-C content RTO samples. We are, however, not able to comment quantitatively on the influence of Ge segregation on the interface state density from the TEM micrographs.

B. SE results

Figure 2 shows the pseudodielectric function versus photon energy for the as-grown $Si_{0.887}Ge_{0.113}$ and $Si_{0.887-y}Ge_{0.113}C_y$ alloys. The large amplitudes of the E_1 and E_2 gaps of these samples indicate good crystallinity of the films. The energy and peak values of ϵ_2 for $Si_{0.887}Ge_{0.113}$ are comparable to strained SiGe films.[12] The amplitudes of ϵ_2 at the E_1 and E_2 gaps decrease with an increase in C concentration. This is due to the alloying effect and stoichiometric deformation of the films. The humps at the lower edge of the E_1 gap at 2.6, 2.4, and 2.3 eV for $Si_{0.8811}Ge_{0.113}C_{0.0059}$, $Si_{0.8738}Ge_{0.113}C_{0.0132}$, and $Si_{0.8686}Ge_{0.113}C_{0.0184}$ films may be due to C-related band gaps.

Figure 3(a) shows the energy dependence of the second derivatives of ϵ_1 and ϵ_2 for the as-grown samples. The results are fitted using the formula develop by Aspnes[13] assuming two critical points, E_1 and E_0'. In general, the agreement between the experimental and the simulated results is good.

Figure 4(a) shows the peak positions of E_1 and E_0' as a function of C concentration for the as-grown samples. The E_1 transition increases linearly with increasing C concentration. The E_0' transition is independent of C concentration. The broadening factor of the E_1 transition for $Si_{0.887}Ge_{0.113}$ is 0.137 eV and increases to 0.149, 0.157, and 0.197 eV with C concentration equal to 0.59%, 1.32%, and 1.84%, respectively. Note that the E_2 peak also broadened but shifts to lower energy. The broadening of the E_1 and E_2 peaks may be attributed to the distortion near the carbon atoms and the internal splitting of electronic bands.[14]

Figure 5 compares ϵ_2 of the as-grown and RTO samples. The intensity of the E_1 and E_2 transitions decreases for all the RTO samples. The E_1 transition shifts towards the lower energy direction for the RTO samples. This means that the transition occurs from a higher Ge content layer in the samples. The higher Ge content layer could be due to the Ge piled up at the SiO_2/substrate interface as a result of RTO. As the E_1 peak for samples $Si_{0.887}Ge_{0.113}$ and

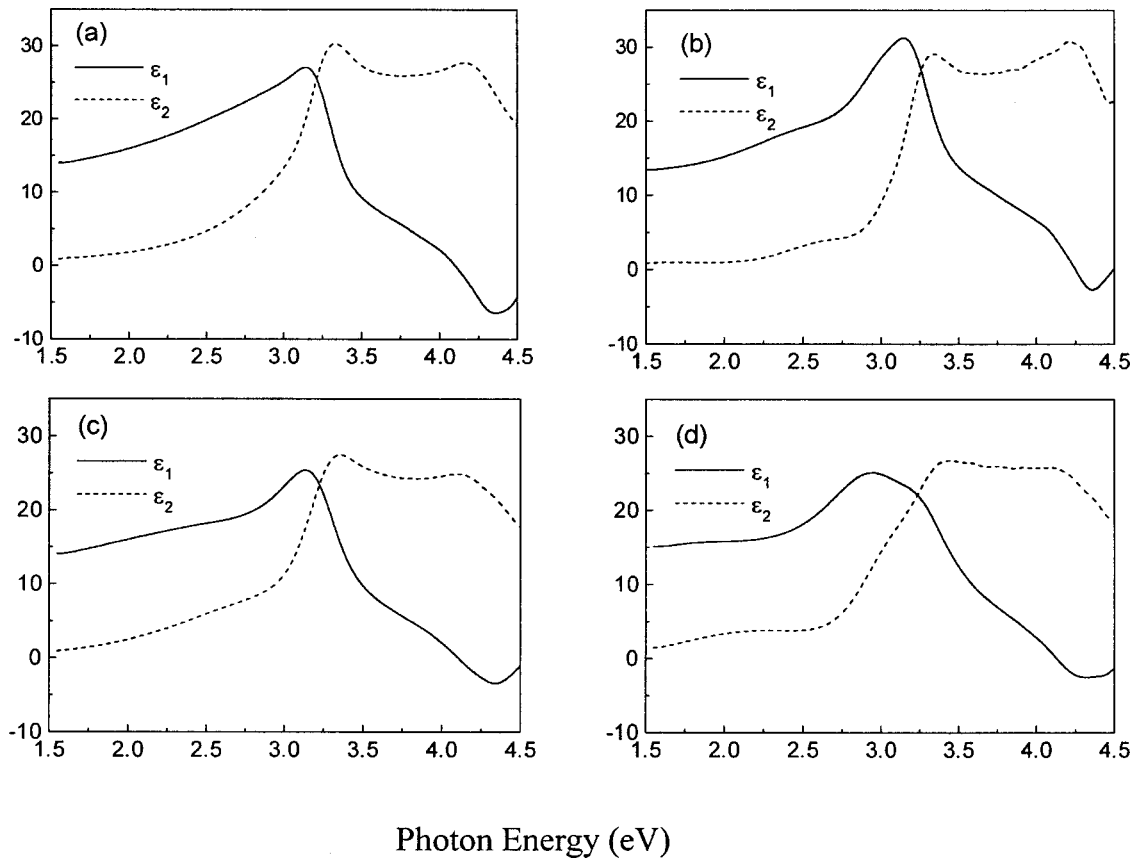FIG. 2. Pseudodielectric function vs photon energy for the as-grown $Si_{0.887}Ge_{0.113}$ and $Si_{0.887-y}Ge_{0.113}C_y$ alloys.

$Si_{0.8811}Ge_{0.113}C_{0.0059}$ are located at 3.07 eV, this means that the RTO process has reduced most of the C in the $Si_{0.8811}Ge_{0.113}C_{0.0059}$ film. For samples $Si_{0.8738}Ge_{0.113}C_{0.0132}$ and $Si_{0.8686}Ge_{0.113}C_{0.0184}$, the E_1 peaks are located at 3.13 and 3.15 eV, respectively. These values are lower than the E_1 peaks of their respective as-grown samples. This suggests a lower C concentration in the RTO samples. This is in good agreement with our previous IR and secondary ion mass spectroscopy (SIMS) results.[6] The large reduction in ϵ_2 intensity at E_2 in Fig. 5 is due to the presence of an oxide layer.

To study the effect of oxidation on our samples, SE measurements were done after the oxide was etched away. The second derivatives of the pseudodielectric function versus photon energy, and the E_1 and E_0' peak versus C content of the etched samples are shown in Figs. 3(b) and 4(b), respectively. As compared to the as-grown samples [Fig. 3(a)], an even better fit between the experimental and theoretical results is obtained for the etched samples. Figure 4(b) shows that the E_1 transition is weakly dependent on the C content. This is reasonable as the C concentrations in the samples were significantly reduced after RTO. With the exception of sample $Si_{0.887}Ge_{0.113}$, the E_0' transition of the etched samples is independent of C content in the film.

It is worthwhile to note that we have observed[5,6] no change in the mismatch strain in the $Si_{0.887}Ge_{0.113}$ film after RTO at 1000 °C for 270 s. Therefore, the reduction in the E_1 value for the RTO $Si_{0.887}Ge_{0.113}$ film is unlikely to be due to strain relaxation. On the other hand, we observed a Ge pileup

of ~16 nm at the SiO_2–SiGe interface after RTO from our SIMS experiments.[15] We have calculated the penetration depth of the light source used in the SE experiments to be ~20 nm. Therefore, we attribute the reduction in the E_1 value in the RTO $Si_{0.887}Ge_{0.113}$ film to be due to the higher Ge concentration layer.[16,17]

For SiGeC films, we found that the strain varied from compressive (C=0.0059), fully compensated (C=0.0132) to tensile (C=0.0184), depending on the carbon concentration in the film. After RTO at 1000 °C for 270 s, the mismatch strain of the $Si_{0.8811}Ge_{0.113}C_{0.0059}$ and $Si_{0.8738}Ge_{0.113}C_{0.0132}$ films increased to a value comparable to the $Si_{0.887}Ge_{0.113}$ film. However, the RTO $Si_{0.8686}Ge_{0.113}C_{0.0184}$ film showed both compressive and tensile strain. Due to the rather complicated patterns in strain for the RTO SiGeC films, it would be inadvisable to discuss the influence of strain on E_1 without further experiments. On the other hand, we discovered a Ge pileup of similar thickness (~16 nm) for SiGeC films at the SiO_2–SiGeC interface after RTO.[7] The reduction in the E_1 values of the RTO SiGeC films may partially be due to the Ge pileup at the interface. Note that our SE results are in complete agreement with that published by Bonan *et al.*[18]

Figure 6 shows the refractive indices of the as-grown and etched samples. It is clear that the refractive index increases with an increase in the incident radiation of less than 3.2 eV. The increase in the refractive index again indicates the presence of a high-Ge content layer in the etched samples.
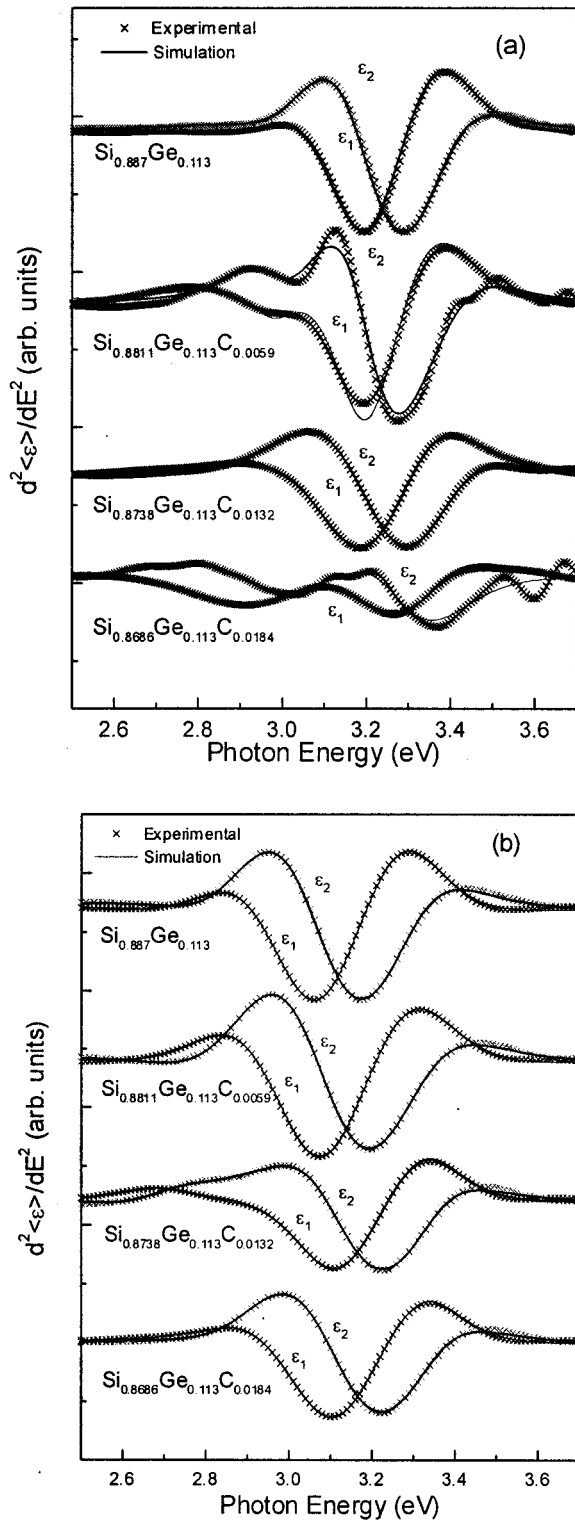
FIG. 3. Second derivatives of the pseudodielectric function of (a) as-grown and (b) RTO samples, with oxide etched away, of $Si_{0.887}Ge_{0.113}$ and $Si_{0.887-y}Ge_{0.113}C_y$ alloys.

C. Electrical results

We have shown previously that rapid thermal oxides grown on $Si_{0.8738}Ge_{0.113}C_{0.0132}$ and $Si_{0.8686}Ge_{0.113}C_{0.0184}$ substrates at $1000\,°C$ were of poor quality.[7] We have shown in Sec. III A that significant SiC precipitation occurred at high-C content $Si_{1-x-y}Ge_xC_y$ samples after $1000\,°C$ oxida-
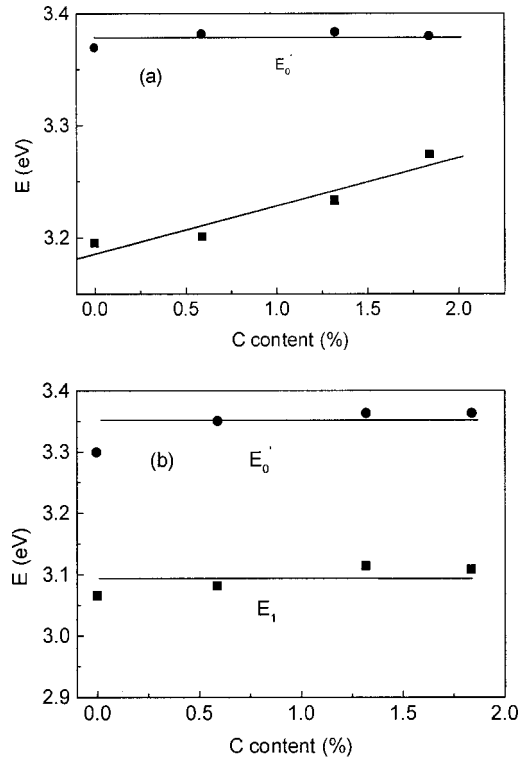

FIG. 4. Energies of the E_1 and E_0' critical points of (a) as-grown and (b) RTO samples, with oxide etched away, of $Si_{0.887}Ge_{0.113}$ and $Si_{0.887-y}Ge_{0.113}C_y$ alloys.

tion. As electrical measurements are nondestructive and simpler in terms of sample preparation, we used the $C-V$ and $I-V$ measurements to explore the possibility of improving the oxide quality. The oxides were grown at a lower RTO temperature of $800\,°C$ in pure O_2 or N_2O ambient for 600 s. The long oxidation time was to ensure reasonable oxide
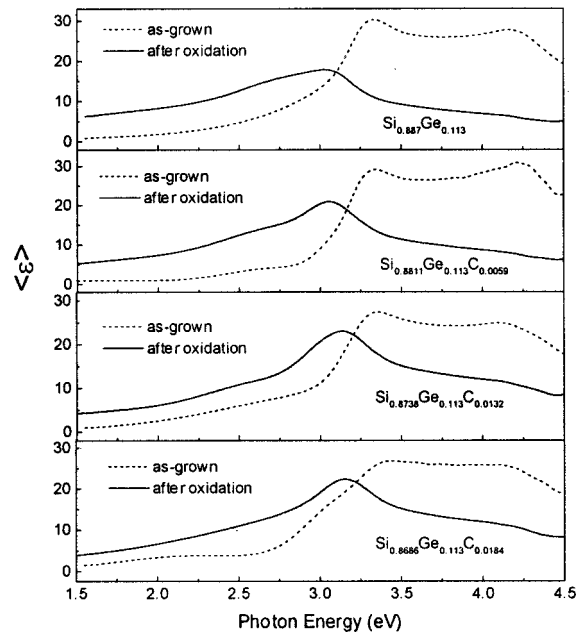

FIG. 5. Imaginary part of the pseudodielectric function of as-grown and RTO $Si_{0.887}Ge_{0.113}$ and $Si_{0.887-y}Ge_{0.113}C_y$ alloys.
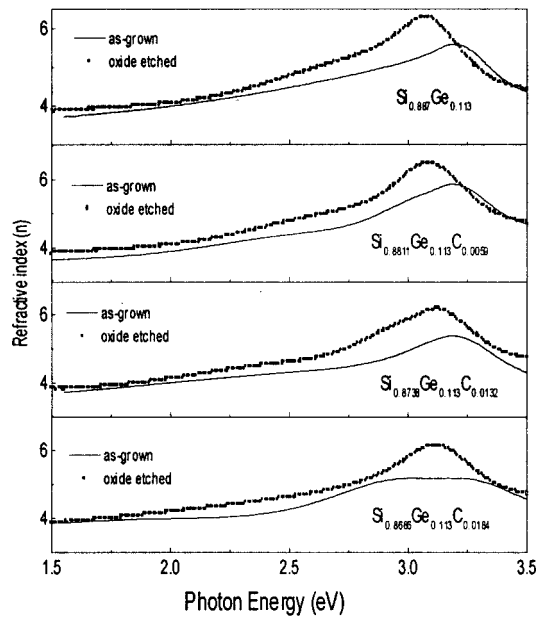
FIG. 6. Refractive indices of as-grown and RTO $Si_{0.887}Ge_{0.113}$ and $Si_{0.887-y}Ge_{0.113}C_y$ alloy films.

FIG. 7. *I–V* characteristics of oxides grown on $Si_{0.887}Ge_{0.113}$ and $Si_{0.8811}Ge_{0.113}C_{0.0059}$ substrates in N_2O or O_2 ambient.

thickness was obtained. We have chosen the $Si_{1-x-y}Ge_xC_y$ substrate with the lowest C content (i.e., $Si_{0.8811}Ge_{0.113}C_{0.0059}$) to minimize SiC precipitation. The electrical results of Al–SiO$_2$–$Si_{0.887}Ge_{0.113}$ capacitors were included for comparison purposes.

We found that thinner oxides were obtained when grown in N_2O ambient as compared to O_2 ambient for both $Si_{0.887}Ge_{0.113}$ and $Si_{0.8811}Ge_{0.113}C_{0.0059}$ substrates (see Table I). This is expected, as oxide growth is always slower in N_2O as compared to O_2.

The *I–V* characteristics of oxides grown on $Si_{0.887}Ge_{0.113}$ and $Si_{0.8811}Ge_{0.113}C_{0.0059}$ substrates in N_2O or O_2 ambient are shown in Fig. 7. The conductivities of oxides (calculated at 4 MV/cm) grown in O_2 (see Table I) are in the range between 1.0×10^{-14} and $2.5 \times 10^{-15} \, \Omega^{-1} \, cm^{-1}$. These are reasonable values as the oxides were grown at a relatively low temperature of 800 °C. We can only observe the Fowler–Nordheim transport mechanism in the $Si_{0.887}Ge_{0.113}$ samples. The onset of Fowler–Nordheim conduction is at ~6 MV/cm. A barrier height of 2.54 eV was obtained from the Folwer–Nordheim plot for the SiO$_2$–$Si_{0.887}Ge_{0.113}$ system. The lower value for the SiO$_2$–$Si_{0.887}Ge_{0.113}$ system (c.f. to the Si–SiO$_2$ system) may be due to the rougher interface.
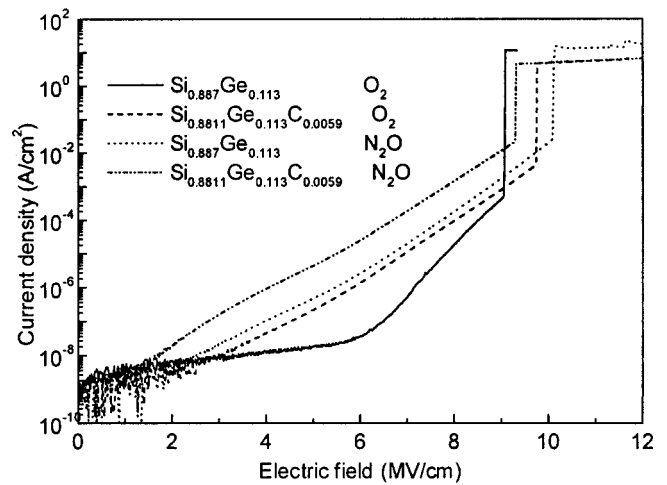
The sample with the $Si_{0.8811}Ge_{0.113}C_{0.0059}$ substrate shows a rapid increase in current for an electric field exceeding 4 MV/cm. It is interesting to note that oxides grown on the $Si_{0.887}Ge_{0.113}$ and $Si_{0.8811}Ge_{0.113}C_{0.0059}$ substrates with N_2O ambient are more leaky ($\sigma = 1.5–2.55 \times 10^{-13} \, \Omega^{-1} \, cm^{-1}$) than the corresponding samples grown in O_2 ambient. Also, the conductivities of the 800 °C oxides are generally 2–3 orders of magnitude higher than the 1000 °C oxides. The breakdown field of the 800 °C oxide on the $Si_{0.887}Ge_{0.113}$ substrate grown in N_2O is higher than that grown in O_2. Note that the breakdown fields for all the oxides grown at 800 °C are significantly lower than the breakdown field (10–14 MV/cm) of oxides grown at 1000 °C.

Figure 8 shows the high-frequency (1 MHz) *C–V* characteristics of the metal–oxide–semiconductor (MOS) structures with $Si_{0.887}Ge_{0.113}$ and $Si_{0.8811}Ge_{0.113}C_{0.0059}$ substrates. The substrate doping concentrations derived from the *C–V* curves are listed in Table I. Taking a relative permittivity of the $Si_{0.887}Ge_{0.113}$ and $Si_{0.8811}Ge_{0.113}C_{0.0059}$ films to be ~12.4, the maximum depletion widths are estimated to be ~400 and 40 nm, respectively. For the $Si_{0.887}Ge_{0.113}$ film, the maximum depletion width will be extended into the Si buffer layer. The Si buffer layer had a doping concentration of 5×10^{15}–$1 \times 10^{16} \, cm^{-3}$. This has resulted in a doping concentration of 5.56×10^{15}–$1.56 \times 10^{16} \, cm^{-3}$ for the RTO $Si_{0.887}Ge_{0.113}$ films. For the RTO $Si_{0.8811}Ge_{0.113}C_{0.0059}$ film, the maximum depletion width is well inside the SiGeC layer. Table I shows

TABLE I. Oxide thickness, conductivity, breakdown field, and the interface state density of RTO oxides grown at 800 °C and the doping concentration on $Si_{0.887}Ge_{0.113}$ and $Si_{0.8686}Ge_{0.113}C_{0.0059}$ substrates. Also included here for comparison are the oxide thickness, conductivity, breakdown field, and interface state density of RTO oxides grown at 1000 °C in O_2 on the same substrates.

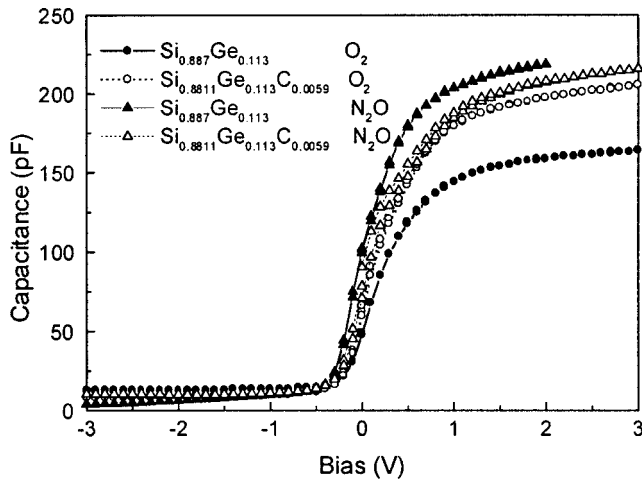| Sample	RTO condition	Oxide thickness (nm)	σ ($\Omega^{-1} \, cm^{-1}$)	E_{bd} (MV/cm)	Doping (cm^{-3})	D_{it} ($cm^{-2} \, eV^{-1}$)
$Si_{0.887}Ge_{0.113}$	O_2 (800 °C)	5.4	2.50×10^{-15}	9.06	1.56×10^{16}	1.62×10^{12}
	N_2O (800 °C)	4.0	2.50×10^{-13}	10.10	5.56×10^{15}	2.42×10^{12}
	O_2 (1000 °C)	17.9	3.98×10^{-16}	12.53	6.70×10^{15}	3.00×10^{11}
$Si_{0.8811}Ge_{0.113}C_{0.0059}$	O_2 (800 °C)	4.3	1.00×10^{-14}	9.75	1.06×10^{16}	2.27×10^{12}
	N_2O (800 °C)	4.1	1.50×10^{-13}	9.30	1.30×10^{16}	2.96×10^{12}
	O_2 (1000 °C)	12.5	7.96×10^{-16}	12.81	5.70×10^{17}	1.10×10^{12}

FIG. 8. High-frequency (1 MHz) $C-V$ characteristics of the MOS structures with $Si_{0.887}Ge_{0.113}$ and $Si_{0.8811}Ge_{0.113}C_{0.0059}$ substrates.

that the $Si_{0.8811}Ge_{0.113}C_{0.0059}$ samples have a higher doping concentration than the $Si_{0.887}Ge_{0.113}$ samples. This agrees with the report of Osten and Gaworzewski[19] in that C in the $Si_{0.8811}Ge_{0.113}C_{0.0059}$ sample would introduce donor-like centers[20] and increase the doping concentration. The doping concentrations of $Si_{0.8811}Ge_{0.113}C_{0.0059}$ samples RTO at 800 and 1000 °C in O_2 are 1.06×10^{16} and 5.7×10^{17} cm^{-3}, respectively. This means that the increase in the doping concentration may also be linked to the formation of SiC precipitates in the films.

The interface state densities (D_{it}) of our samples, calculated from the Hill and Coleman method,[21] are listed in Table I. Note that these D_{it} values were obtained at a depletion width (31–69 nm for $Si_{0.887}Ge_{0.113}$ and 20–33 nm for $Si_{0.8811}Ge_{0.113}C_{0.0059}$ samples), well within the thickness of the $Si_{0.887}Ge_{0.113}$ and $Si_{0.8811}Ge_{0.113}C_{0.0059}$ layers. Significant higher D_{it} values (1.62–2.96×10^{12} eV^{-1} cm^{-1}) were obtained for the 800 °C oxides. The D_{it} values of oxides grown at 1000 °C with the $Si_{0.887}Ge_{0.113}$ and $Si_{0.8811}Ge_{0.113}C_{0.0059}$ substrates are 3.0×10^{11} and 1.1×10^{12} eV^{-1} cm^{-1}, respectively. We can, therefore, conclude that a lower oxidation temperature is not suitable in reducing D_{it}. We have used the metal work function between Al and Si to estimate the Q_f values of the MOS structure with oxide grown at 800 and 1000 °C on the $Si_{0.887}Ge_{0.113}$ substrate to be -1.14×10^{12} and -9.5×10^{11} cm^{-2}, respectively. This again indicates that a lower oxidation temperature resulted in a higher fixed charge value in the oxide. Ahn *et al.*[22] have suggested that the negative fixed charge observed in the SiGe system was a result of Si–O– dangling bonds in the oxide. The larger Q_f value in the 800 °C (as compared to the 1000 °C sample) may be due to the higher amount of Si–O– dangling bonds that exist in the oxide. We are not able to compare the Q_f results of the $Si_{0.8811}Ge_{0.113}C_{0.0059}$ samples as the 1000 °C showed a rather abnormal trend with the C content in the film.

IV. CONCLUSIONS

The TEM results showed a significant SiC precipitation in the high-C content $Si_{1-x-y}Ge_xC_y$ sample after RTO. The

SE results showed that the E_1 gap increased and E_2 gap decreased as the C concentration increased. For the RTO samples, the amplitude of the E_2 transitions reduced rapidly and the E_1 transition shifted to a lower energy. The reduction of the amplitude of the E_2 transitions is due to the presence of the oxide layer. The refractive indices of the RTO samples were higher compared to the as-grown films. A high-Ge content layer and the low-C content in the RTO films accounted for the E_1 shift to lower energy and the increase of the refractive index. We conclude from the electrical measurements that RTO at a lower temperature of 800 °C did not improve the oxide quality as compared to 1000 °C.

[1] G. L. Patton *et al.*, IEEE Electron Device Lett. **11**, 171 (1990).
[2] R. Karunasiri, J. S. Park, and K. L. Wang, Appl. Phys. Lett. **59**, 2588 (1991).
[3] Y. Rajakarumamayake and T. McGill, J. Vac. Sci. Technol. B **8**, 929 (1990).
[4] Y. Mii, Y. Xie, E. Fitzgerald, D. Monroe, F. Thiel, B. Weir, and L. Feldman, Appl. Phys. Lett. **59**, 1611 (1991).
[5] W. K. Choi, L. K. Bera, J. H. Chen, W. Feng, K. L. Pey, H. Yoong, J. Mi, F. Zhang, and C. Y. Yang, Mater. Sci. Eng., B **75**, 184 (2000).
[6] W. K. Choi, J. H. Chen, L. K. Bera, W. Feng, K. L. Pey, J. Mi, C. Y. Yang, A. Ramam, S. J. Chua, J. S. Pan, A. T. S. Wee, and R. Liu, J. Appl. Phys. **87**, 192 (2000).
[7] L. K. Bera, W. K. Choi, W. Feng, C. Y. Yang, and J. Mi, Appl. Phys. Lett. **77**, 256 (2000).
[8] J. Mi, P. Warren, P. Letourneau, M. Judelewicz, M. Gaihanou, M. Dutoit, C. Dubois, and J. C. Dupuy, Appl. Phys. Lett. **67**, 259 (1995).
[9] P. Warren, J. Mi, F. Overney, and M. Dutoit, J. Cryst. Growth **157**, 414 (1995).
[10] A. Cuadras, B. Carrido, C. Bonafos, J. R. Morante, L. Fonseca, and K. Pressel, Microelectron. Reliab. **40**, 829 (2000).
[11] J. W. Strane, H. J. Stein, S. R. Lee, S. T. Picraux, J. K. Watanabe, and J. W. Mayer, J. Appl. Phys. **76**, 3656 (1994).
[12] H. Lee, Thin Solid Films **313-314**, 167 (1998).
[13] D. E. Aspnes, in *Handbook on Semiconductors* (North-Holland, Amsterdam, 1980), Vol. 2, p. 109.
[14] B. Dietrich, H. J. Osten, H. Rucker, M. Methfessel, and P. Zaumseil, Phys. Rev. B **49**, 17185 (1994).
[15] J. H. Chen, MEng thesis, National University of Singapore (1999).
[16] J. Humlicek, M. Garriga, M. I. Alonso, and M. Cardona, J. Appl. Phys. **65**, 2827 (1989).
[17] C. Pickering, R. T. Carline, D. J. Robbins, W. Y. Leong, S. J. Barnett, A. D. Pitt, and A. G. Cullis, J. Appl. Phys. **73**, 239 (1993).
[18] J. Bonan, F. Meyer, E. Finkman, P. Warren, and P. Boher, Thin Solid Films **364**, 53 (2000).
[19] H. J. Osten and P. Gaworzewski, J. Appl. Phys. **82**, 4977 (1997).
[20] B. Carrido, J. Morante, M. Franz, K. Pressel, D. Krüger, P. Zaumseil, and H. J. Osten J. Appl. Phys. **85**, 833 (1999).
[21] W. A. Hill and C. C. Coleman, Solid-State Electron. **23**, 987 (1980).
[22] C. G. Ahn, H. S. Kang, Y. K. Kwon, S. M. Lee, B. R. Ryum, and B. K. Kang, J. Appl. Phys. **86**, 1542 (1999).